Int. J. Solids Structures Vol. 24, No. 7, pp. 659–673, 1988
Printed in Great Britain.

0020-7683/88 $3.00 + .00

STRAIN-SOFTENING BAR AND BEAM: EXACT NON-LOCAL SOLUTION

ZDENĚK P. BAŽANT and ALEKSANDER ZUBELEWICZ
Department of Civil Engineering, Technological Institute, Northwestern University, Evanson, IL 60201, U.S.A.

(*Received* 19 *November* 1986; *in revised form* 20 *June* 1987)

Abstract—Using the recently developed imbricate non-local continuum approach, zones of strain softening (distributed microcracking) which have a finite size can be modeled. A differential approximation of the averaging integrals for the non-local continuum makes it possible to obtain exact analytical solutions for uniaxial softening in a bar or for flexural softening in a beam. The differential equations of the problem along with the essential and natural boundary conditions and the conditions at the interface between the softening and non-softening regions are derived by a variational procedure based on the principle of virtual work. The failure due to strain softening is analyzed as a stability problem. In contrast to the blunt crack band model, the size of the strain-softening region is treated as an unknown to be solved by stability analysis. Numerical results show that the size of the strain-softening region is approximately constant, and so is the energy dissipated due to failure. Ductility diagrams, giving the strain at failure as a function of beam size and support stiffness are also calculated and are found to be quite similar to those obtained previously by local analysis with an assumed size of the softening region. These conclusions lend further support to the use of a blunt crack band model for localized cracking.

INTRODUCTION

Failure of brittle heterogeneous materials such as concrete or rock usually involves large zones of distributed cracking. On the macroscale, the material in these zones exhibits strain softening, i.e. a gradual decrease of stress at increasing strain. The mathematical modeling of this phenomenon has recently generated extensive debate[1–3]. Problems arise with the strain-softening concept when a rate-independent local continuum is considered. For that case, it may be shown that strain-softening zones of finite size are in general unstable, and the cracking or strain softening may localize to a zone of zero volume, i.e. a surface, or a line, or a point. Nevertheless, large zones of cracking are often observed experimentally.

A simple way to describe cracking zones of finite size in a finite element code is to prescribe the minimum size of the strain-softening finite elements. This approach, proposed on the basis of stability analysis in 1974[4], has led to the formulation of the blunt crack band model[4–7], which has been shown to be in agreement with the fracture test data on concrete or rock available in the literature. An alternative method to obtain agreement with these fracture data is to lump the cracking into a line and postulate a stress–displacement relation at the tip of a line crack[8], in a manner which is similar to the original models for the cohesive zone in ductile fracture[9, 10]. This alternative approach, however, is incapable of handling cracking situations in which the cracking does not localize to a zone of minimum possible width, as determined by the aggregate size or grain size, but remains distributed over much larger areas. Such situations happen, e.g. in reinforced concrete when the steel ratio is sufficiently large, or in dynamics where inertial forces prevent immediate localization, and also in certain situations where a compression zone immediately ahead of the fracture front provides a restraint which prevents the localization of cracking, as has been demonstrated for certain thermal stress problems.

A rigorous formulation for distributed cracking, which has the blunt crack band model as its special case and can describe strain-softening zones of finite size, was recently proposed in Ref. [6]. Like the classical non-local continuum theory[11–15], the macroscopic stress, called broad-range stress, is considered to be a function of the mean strain over a certain representative volume the size of which (the characteristic length) is a property of the material. Unlike the classical non-local continuum theory, however, the averaging operator that defines the mean strain must be applied once more to the broad-range stress in

order to obtain the stress to be substituted into the differential equation of equilibrium. Furthermore, this non-local continuum must be coupled in parallel (i.e. overlaid) with a local continuum in which the (local) stress at a point depends only on the strain at the same point. This overlay is necessary to prevent spurious zero-energy periodic deformation modes. The continuum may be considered as the limiting case of a system of imbricated (regularly overlapping) finite elements the size of which is kept constant and equal to the characteristic length of the medium while the mesh is refined. Therefore, this new type of non-local continuum is called imbricate.

The imbricate non-local continuum has so far been used only in numerical finite element studies. Various problems of one-dimensional planar, cylindrical, and spherical waves as well as the fracture process in a two-dimensional rectangular specimen have been solved for strain-softening materials. However, no exact analytical solutions for the imbricate non-local continuum have yet been obtained. Development of such solutions is the objective of this work. Such solutions are useful for verification and calibration of imbricate non-local finite element programs. They can also bring to light some simple basic properties of the imbricate non-local continuum, e.g. the variation of the size of the strain-softening domain and the energy dissipated in it as a function of the structure size, support stiffness, and the softening slope of the macroscopic stress–strain diagram. We will demonstrate such solutions for one-dimensional problems of axial deformation as well as bending.

Before embarking on our analysis, it is proper to mention that some researchers at present believe that continuum models with strain softening, even in the recent non-local form, do not adequately describe the physical reality. Some of them assert that the only realistic approach is either micromechanics analysis introducing some specific form of material inhomogeneities or representation of a damage zone through a softening stress–displacement relation for an isolated equivalent crack. Others propose the use of homogenization theory, although questions then arise whether homogenization is physically realistic if discontinuities can develop within the softening zone or on its boundary. Interesting though such proposals and criticisms may be, they have not so far led to any usable mathematical model for structural analysis. Within the limited scope of this paper, these divergent views cannot be analyzed adequately. For a more detailed discussion see, e.g. Ref. [1] which gives an extensive bibliography.

It is proper to point out also that another formulation of a non-local continuum for strain softening has been found after the completion of the present analysis[16–18]. This formulation in which the elastic strains are considered to be local and the non-local treatment is applied only to those internal variables which cause strain softening, has been found to perform very well in finite element analysis and has already been successfully applied to a finite element system with several thousand nodal displacements[16] (e.g. problems of stability of the excavation of a tunnel in a grouted strain-softening soil). The advantages of this alternative formulation are that: (1) it requires no element imbrication and thus is simpler to program, (2) no extra boundary conditions of higher order (such as eqns (13)–(15)) are needed, and (3) there exist no periodic zero-energy instability modes, making an overlay with a local elastic continuum unnecessary. This alternative formulation, however, does not apparently permit explicit analytical solutions such as presented in this paper. Also, the operators in it are not symmetric, while those in the present formulation are.

DIFFERENTIAL APPROXIMATION FOR A NON-LOCAL CONTINUUM BAR

We consider a bar of uniform cross section with a unit area (Fig. 1(c)). The bar is initially in equilibrium at initial total stress S^0 and initial axial displacements $u^0(x)$ which depend on the axial coordinate x. We consider increments $u(x)$ of the axial displacement from this initial state. In the imbricate non-local continuum, we must distinguish two kinds of incremental stresses: the local stress τ and the broad-range stress σ, which may be expressed as

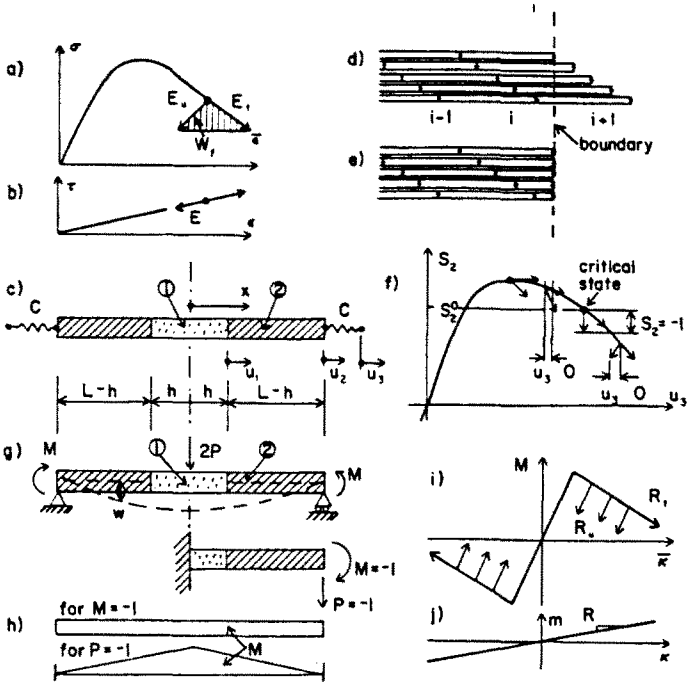

Fig. 1. Stress–strain and moment–curvature diagrams, and notations for a uniaxially loaded bar.

$$\tau = E\frac{\mathrm{d}u}{\mathrm{d}x}, \quad \sigma = \bar{E}\bar{\varepsilon}, \quad \bar{\varepsilon}(x) = \int_{l/2}^{l/2} \alpha(s)\frac{\mathrm{d}u(x+s)}{\mathrm{d}x}\,\mathrm{d}s \tag{1}$$

in which E, $\bar{E}$ are the local and non-local incremental elastic moduli, $\mathrm{d}u/\mathrm{d}x = \varepsilon$ the local strain increments, $\bar{\varepsilon}$ the mean (or non-local) strain increment, $\alpha(s)$ the given empirical weighting function, and l the characteristic length, over which the strain averaging is carried out.

The integral definition of the mean strain in eqn (1) makes it difficult to obtain analytical solutions. It also requires modification at points closer to the ends of the bar than $l/2$. Therefore, we will use a differential approximation (2), which is obtained by expanding $u(x)$ into a Taylor series, integrating and truncating the resulting series after the second term; this leads to

$$\bar{\varepsilon} = \left(1 + \lambda^2\frac{\mathrm{d}^2}{\mathrm{d}x^2}\right)\frac{\mathrm{d}u}{\mathrm{d}x} \tag{2}$$

in which λ is the length constant (equal to $l/\sqrt{24}$ if $\alpha = 1$; see Ref. [5]). It may be shown by variational calculus (2) that the differential equation of equilibrium associated with eqn (2) must have the form $\mathrm{d}S/\mathrm{d}x = 0$ in which S is the total stress (i.e. the actual stress), defined as

$$S = (1-c)\bar{\sigma} + c\tau, \quad \bar{\sigma} = \left(1 + \lambda^2\frac{\mathrm{d}^2}{\mathrm{d}x^2}\right)\sigma \tag{3}$$

where $\bar{\sigma}$ is the mean stress and c the empirical coefficient characterizing the fraction of the local response. For $c = 1$ all response is local, and for $c = 0$ all response would be nonlocal. However, as shown before eqn (2), the case $c = 0$ is unstable (for a uniform weighting function $\alpha(s)$), permitting periodic zero energy deformation modes. Stability requires that $c > 0$, although for practical numerical reasons the values of c less than about 0.1 should be avoided in finite element analysis because they produce excessive numerical noise.

The material of the bar is assumed to obey a rate-independent stress–strain relation

which exhibits a post-peak strain softening (Fig. 1(a)). As shown before eqns (1) and (2), the strain softening is admissible only for the non-local part of material behavior, i.e. for the dependence of the broad-range stress σ on the mean strain $\bar{\varepsilon}$. The local behavior may be elastic (Fig. 1(b)) or elastic–plastic hardening, but not softening. For the non-local inelastic behavior, we must distinguish the incremental elastic moduli for further loading (increasing strain), $\bar{E} = E_t$, and for unloading (decreasing strain), $\bar{E} = E_u$. For the pre-peak, hardening regime, $E_t > 0$, while for the post-peak, softening regime, $E_t < 0$. Always $E_u > 0$. For the local behavior, $E > 0$ always.

We consider only static deformations, in which the bar must be in equilibrium, and so $S = \text{const.}$ along the bar. When the broad-range stress is in the pre-peak hardening regime, only one strain value corresponds to a given stress value, and so the strain distribution must be uniform. For the post-peak softening behavior, however, the strain does not have to be uniform because more than one strain value is associated with a given stress value. Accordingly, we assume that a centrally located segment of length $2h$ undergoes further loading, and the remaining segments of lengths $L-h$ undergo unloading from the same initial state characterized by stresses τ^0, σ^0, S^0 and strains $\varepsilon^0 = \bar{\varepsilon}^0$ (Fig. 1(c)). (It may be shown that strain softening always localizes into a single segment rather than several segments.) To simulate the behavior of a specimen in a testing machine, we consider the specimen to be loaded through springs of spring constants C attached at the ends.

Due to symmetry, we analyze only one-half of the bar of length L, loaded by one spring. The objective of our analysis is to check successive post-peak states in the strain-softening regime and determine the initial strain ε^0 at which the strain distribution first becomes unstable, with strain localization into a segment of length h. This length is also unknown and is to be solved. The bar is loaded at the end of the spring in a displacement controlled fashion, and the strain increments ε are assumed to happen so rapidly that the displacement at the end of the spring is zero, i.e. no work is done by the external loads or prescribed displacements during the incremental deformation.

The essential and natural boundary conditions were determined before[2], but the interface conditions and the conditions for elastic boundary restraint or symmetry were not. To obtain these conditions, we consider the virtual work of the incremental stresses in the system

$$\delta W = \int_0^L (1-c)\sigma\delta\bar{\varepsilon}\,\mathrm{d}x + \int_0^L c\tau\varepsilon\,\mathrm{d}x + \delta W_L = 0$$
$$\delta W_L = C[u_3 - u_2(L)]\,[\delta u_3 - \delta u_2(L)] \tag{4}$$

in which $u_2(L)$ is the displacement at the end $x = L$ of the bar, and u_3 is the displacement at the end of the attached spring. The stiffness C of the spring is assumed to be constant. Distinguishing the stresses and displacements in the loading and unloading segments by subscripts 1 and 2, and substituting eqn (2) for $\bar{\varepsilon}$ with $\varepsilon = \mathrm{d}u/\mathrm{d}x = u'$, we obtain

$$\delta W = \int_0^h [(1-c)\sigma_1(\delta u_1' + \lambda^2\delta u_1''')]\,\mathrm{d}x + \int_h^L [(1-c)\sigma_2(\delta u_2' + \lambda^2\delta u_2''')]\,\mathrm{d}x$$
$$+ \int_0^h c\tau_1\delta u_1'\,\mathrm{d}x + \int_h^L c\tau_2\delta u_2'\,\mathrm{d}x + \delta W_L = 0 \tag{5}$$

in which the primes are used to denote the derivatives with respect to x. Through successive integrations by parts we may transform eqn (5) as follows:

$$\delta W = [(1-c)\sigma_1(\delta u_1 + \lambda^2\delta u_1'') + c\tau_1\delta u_1]_0^h$$
$$- \int_0^h [(1-c)\sigma_1'(\delta u_1 + \lambda^2\delta u_1'') + c\tau_1'\delta u_1]\,\mathrm{d}x + [(1-c)\sigma_2(\delta u_2 + \lambda^2\delta u_2'') + c\tau_2\delta u_2]_h^L$$
$$- \int_h^L [(1-c)\sigma_2'(\delta u_2 + \lambda^2\delta u_2'') + c\tau_2'\delta u_2]\,\mathrm{d}x + \delta W_L = 0 \tag{6}$$

$$\delta W = [[(1-c)(\sigma_1+\lambda^2\sigma_1'')+c\tau_1]\delta u_1]_0^h+[(1-c)\lambda^2(\sigma_1\delta u_1''-\sigma_1'\delta u_1')]_0^h$$

$$-\int_0^h [(1-c)(\sigma_1+\lambda^2\sigma_1'')+c\tau_1]'\,\delta u_1\,\mathrm{d}x+[[(1-c)(\sigma_2+\lambda^2\sigma_2'')+c\tau_2]\delta u_2]_h^L$$

$$+(1-c^2)\lambda[\sigma_2\delta u_2''-\delta_2'\sigma u_2']_h^L-\int_h^L [(1-c)(\sigma_2+\lambda^2\sigma_2'')+c\tau_2]'\delta u_2\,\mathrm{d}x+\delta W_L=0 \quad (7)$$

$$\delta W = [S_1\delta u_1]_0^h+[(1-c)\lambda^2(\sigma_1\delta u_1''-\sigma_1'\delta u_1')]_0^h-\int_0^h S_1'\delta u_1\,\mathrm{d}x$$

$$+[S_2\delta u_2]_h^L+[(1-c)\lambda^2(\sigma_2\delta u_2''-\sigma_2'\delta u_2')]_h^L-\int_h^L S_2'\delta u_2\,\mathrm{d}x+\delta W_L=0. \quad (8)$$

The condition that this variational equation must be satisfied for any kinematically admissible variations $\delta u_1(x)$ and $\delta u_2(x)$ yields:

differential equilibrium equations

$$\frac{\mathrm{d}S_1}{\mathrm{d}x}=(1-c)E_t\left(1+\lambda^2\frac{\mathrm{d}^2}{\mathrm{d}x^2}\right)^2\frac{\mathrm{d}u_1^2}{\mathrm{d}x^2}+cE\frac{\mathrm{d}u_1^2}{\mathrm{d}x^2}=0$$

$$\frac{\mathrm{d}S_2}{\mathrm{d}x}=(1-c)E_u\left(1+\lambda^2\frac{\mathrm{d}^2}{\mathrm{d}x^2}\right)^2\frac{\mathrm{d}u_2^2}{\mathrm{d}x^2}+cE\frac{\mathrm{d}u_2^2}{\mathrm{d}x^2}=0; \quad (9)$$

boundary conditions of symmetry at $x=0$

$$S_1'\delta u_1=0,\quad \sigma_1'\,\delta u_1'=0,\quad \sigma_1\,\delta u_1''=0; \quad (10)$$

interface conditions at $x=h$

$$S_1\delta u_1=S_2\delta u_2,\quad \sigma_1'\delta u_1'=\sigma_2\delta u_2',\quad \sigma_1\delta u_1''=\sigma_2\delta u_2''; \quad (11)$$

boundary conditions at $x=L$

$$\sigma_2\delta u_2''=\sigma_2'\delta u_2',\quad \{S_2+C[u_3-u_2(L)]\}\delta u_2(L)=0. \quad (12)$$

The foregoing conditions imply both the natural (static) and the essential (kinematic) boundary or interface conditions. We must now choose between the two and we do so as follows:

for $x=0$

$$u_1=0,\quad u_1''=0,\quad \sigma_1'=0\ (\text{or } u_1^{\mathrm{IV}}=0); \quad (13)$$

for $x=h$

$$u_1=u_2,\quad u_1'=u_2',\quad u_1''=u_2'',\quad S_1=S_2,\quad \sigma_1=\sigma_2,\quad \sigma_1'=\sigma_2'; \quad (14)$$

for $x=L$

$$S_2=[u_3-u_2(L)],\quad \sigma_2'=0,\quad u_2''=0. \quad (15)$$

Equations (13) give the boundary conditions which satisfy the requirements of symmetry of the displacement field with regard to the middle of the bar and the condition that strain

ε should be nonzero at $x = 0$. Note that the conditions $\sigma_1' = 0$ and $u_1'' = 0$ at $x = 0$ imply $u^{IV} = 0$, which could replace the boundary condition $\sigma_1' = 0$ at $x = 0$.

Equations (14) and eqns $(15)_2$ and $(15)_3$ can also be derived physically if one considers the imbricate microstructure as described in Ref. [4]. At each point of the bar there are infinitely many infinitely thin elements of length l overlapping each other (Fig. 1(d)), and the end of the bar the imbricated elements protruding beyond $x = L$ are chopped off and anchored at $x = L$ (Fig. 1(e)). The corresponding difference equations agree in the limit with eqns (14) and (15).

The differential equations in eqns (9) for segments $0 \leqslant x < h$ and $h \leqslant x \leqslant L$ are of the sixth order and, therefore, their general solution involves 12 arbitrary constants. This agrees with the number of boundary and interface conditions in eqns (13)–(15), which is also 12.

SOLUTION OF DIFFERENTIAL EQUATIONS

Since c, E, E_u and E_t are constants within the unloading and softening segments, and $E_t < 0$ with the other constants being positive, the general solution of eqns (9) may be written as

$$u_1(x) = B_1 \sin \alpha_1 x + B_2 \sin \beta_1 x + B_3 \cos \alpha_1 x + B_4 \cos \beta_1 x + B_5 x + B_6 \tag{16}$$

and

$$u_2(x) = C_1 \cosh \alpha_2 x \sin \beta_2 x + C_2 \sinh \alpha_2 x \cos \beta_2 x + C_3 \cosh \alpha_2 x \cos \beta_2 x + C_4 \sinh \alpha_2 x \sin \beta_2 x + C_5 x + C_6 \tag{17}$$

$$\alpha_1 = \lambda^{-1}(1 + A_1)^{1/2}, \quad B_1 = \lambda^{-1}(1 - A_1)^{1/2}, \quad A_1 = (cE)^{1/2}[-(1-c)E_t]^{-1/2} \tag{18}$$

and

$$\alpha_2 = \lambda^{-1}(A_3 - \tfrac{1}{2})^{1/2}, \quad \beta_2 = \lambda^{-1}(A_3 + \tfrac{1}{2})^{1/2}, \quad A_3 = [\tfrac{1}{2}(1 + A_2)]^{1/2}, \quad A_2 = cE[(1-c)E_u]^{-1}. \tag{19}$$

Substitution of these equations into the boundary and interface conditions in eqns (13)–(15) yields a system of 12 algebraic linear equations for the unknown constants $B_1, B_2, \ldots, B_6$, $C_1, \ldots, C_6$. Solution of this linear equation system was programmed for a computer.

STRAIN-LOCALIZATION INSTABILITY

To check for stability, we may apply the procedure first used in Ref. [4] in 1974 in an analysis of the same problem for a local medium. The system is stable if the work that must be done on the system to produce any admissible kinematical variation of displacements is positive. Thus, if this work is not done, no displacement variation occurs, i.e. the system is stable. However, if at least for one kinematically admissible displacement variation this work is negative, the displacement variation will happen spontaneously and energy will be released. This is an unstable situation. The case when the work is zero is the critical state.

One type of incremental loading which obviously tends to induce strain localization is to enforce displacement δu at the interface $x = h$ between the softening and loading segments, the end of the spring being held fixed ($u_3 = 0$). If the reaction δU at $x = h$ is positive, the work $\Delta W = \delta Q\, \delta u/2$ is positive, and so the system is stable. Otherwise it is unstable.

At the critical state $\delta u = 0$, i.e. the reaction variation is zero while the displacement variations are nonzero. These displacement variations are accompanied by a change of stress $S_2(L)$ in the spring. Thus, the critical state is characterized by the possibility of a change of the end reaction in the spring at no change of end displacement. This means that on approach to instability the incremental stiffness for end loading of the system tends to

infinity, or that the incremental compliance tends to zero. If the incremental compliance is positive, the system is stable, and if it is negative, the system in unstable. This method of detecting instability is used in our numerical calculations.

We assume that the broad range stress–strain diagram in Fig. 1(b) is given, which means that the tangent modulus for loading, E_t, is known as a function of strain $\bar{\varepsilon}$. Also given is the unloading modulus E_u as a function of $\bar{\varepsilon}$ (Fig. 1(b)). The elastic modulus E for local behavior is specified, too, and so are the length L of the bar, the spring constant C, and the material characteristic length λ.

At which value of strain $\bar{\varepsilon}$ does the system become unstable? This question may be answered by the following numerical procedure in which stability is checked for a sequence of increasing discrete values $\bar{\varepsilon}_i^0$ $(i = 1, 2, 3, \ldots)$ of initial strain $\bar{\varepsilon}^0$, and for each $\bar{\varepsilon}_i^0$ for a sequence of increasing values h_j $(j = 1, 2, \ldots, N)$ of segment h.

(1) Loop on initial strain values $\bar{\varepsilon}^0$ of a uniform initial strain in the bar, increasing from 0 to a certain specified maximum value (e.g. 5) ε_t, where ε_t is the strain at peak stress.

(2) For the $\bar{\varepsilon}_i^0$, determine E_t and E_u as specified.

(3) Loop on discrete values h_j, increasing in discrete steps from 0 to L $(j = 1, 2, \ldots, N)$.

(4) Solve $B_1, B_2, \ldots, C_1, \ldots, C_6$, and u_3 from the boundary conditions in eqns (13)–(15) in which $S_2(L) = -1$.

(5) If $u_3 \leqslant 0$, go to step 7. Otherwise return to step 3 and repeat steps 3–5 for the next h-value.

(6) No h-value gives a critical state for this $\bar{\varepsilon}_i^0$-value. Return to step 1 and repeat steps 1–5 for the next $\bar{\varepsilon}_i^0$-value.

(7) Now $u_3 \leqslant 0$. So the critical value of h is between the last two values h_j. Interpolate, using Newton iterations, to determine the critical h more accurately.

(8) Then repeat these iterations for various values of $\bar{\varepsilon}^0$ lying between the last two discrete values of $\bar{\varepsilon}_i^0$. This involves repetition of steps 1–3 for intermediate discrete values of $\bar{\varepsilon}^0$ in order to determine the critical value of $\bar{\varepsilon}^0$ more accurately, along with the corresponding h.

Normally $h < L$, except for very small beam lengths. Then the smallest $\bar{\varepsilon}^0$ for which a critical state exists is characterized by two simultaneous conditions: $u_3(h_1\bar{\varepsilon}^0) = 0$ and $\partial u_3(h_1\bar{\varepsilon}^0)/\partial h = 0$ for $S_2(L) = -1$. The foregoing algorithm is one way to solve these conditions, but other numerical root search methods can be employed just as well. However, if $u_3 = 0$ occurs for $h = L$, which may happen for very small L, then the condition $\partial u_3/\partial h = 0$ need not apply.

The results of numerical calculations are plotted in Figs 2–5. Figure 2 shows an example of the dependence of the length of the strain-softening segment, $2h$, on the length

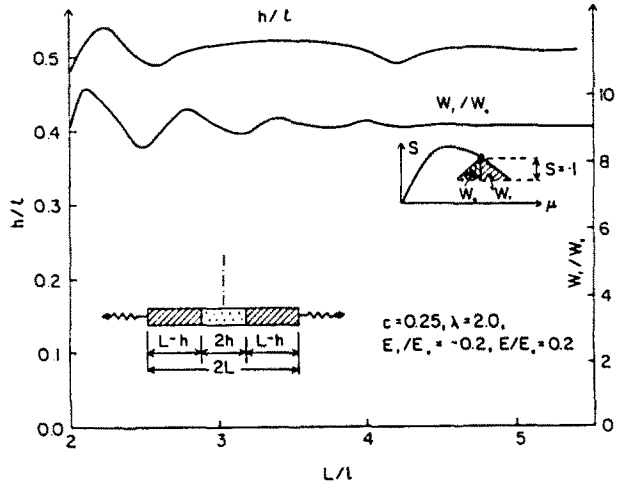

Fig. 2. Dependence of length h of strain-softening segment (left scale) and of dissipated energy W_r (right scale) on length L.

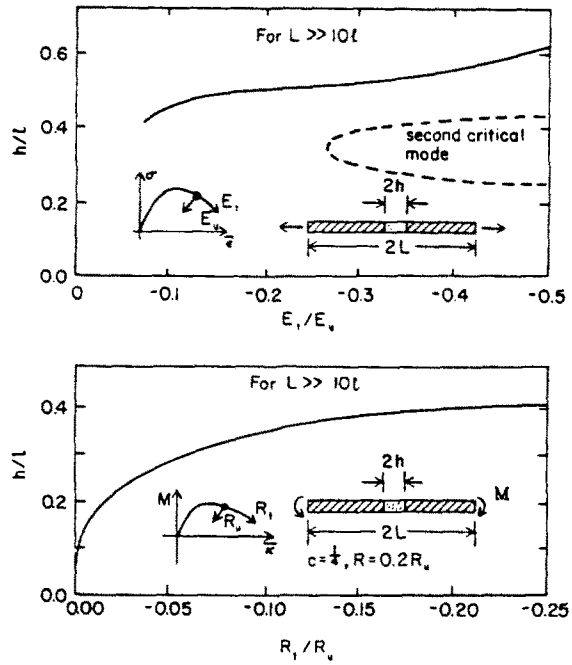

Fig. 3. Length h of strain-softening segment as a function of the strain-softening modulus E_t (top) and of softening bending rigidity R_t (bottom).

of the bar, normalized with regard to the characteristic length l ($l^2 = 24\lambda^2$). The spring is considered infinitely stiff, the ratio of the loading and unloading non-local moduli is $E_t/E_u = -0.2$, the local elastic modulus is $E = 0.2E_u$, and the non-local participation factor is $c = 0.25$. We see that the length of the localization segment is not constant, but it may be considered as approximately constant, in this case $2h \approx 1.2l$. This agrees with the assumption made in the crack band model, eqn (6).

Figure 2 also shows how the energy, W_f, dissipated in the strain-softening zone depends on the relative length of the beam, for which $C \to 0$. The density of W_f (i.e. energy dissipated per unit length of the bar) is defined by the cross-hatched area in the broad-range stress–strain diagram in Fig. 1(b) (the reason that this represents the dissipated energy, or the fracture energy, is given in Ref. [6] or Ref. [2]). W_f is normalized with respect to the elastic energy $hS^2/2E_u$. Note that, except for some initial fluctuation, the dissipated energy, which is essentially equivalent to the fracture energy, is approximately independent of the relative

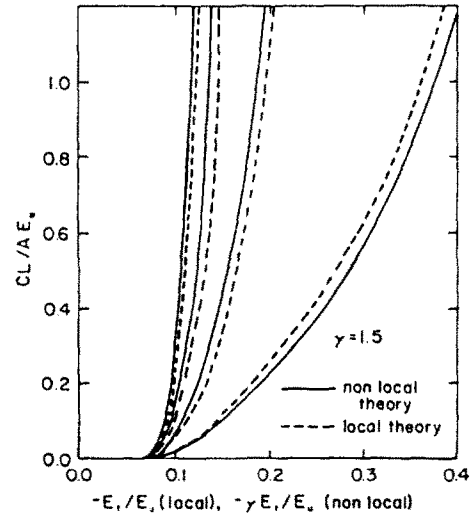

Fig. 4. States of strain localization on instability for non-local theory and for local theory with length γh of strain-localization segment.

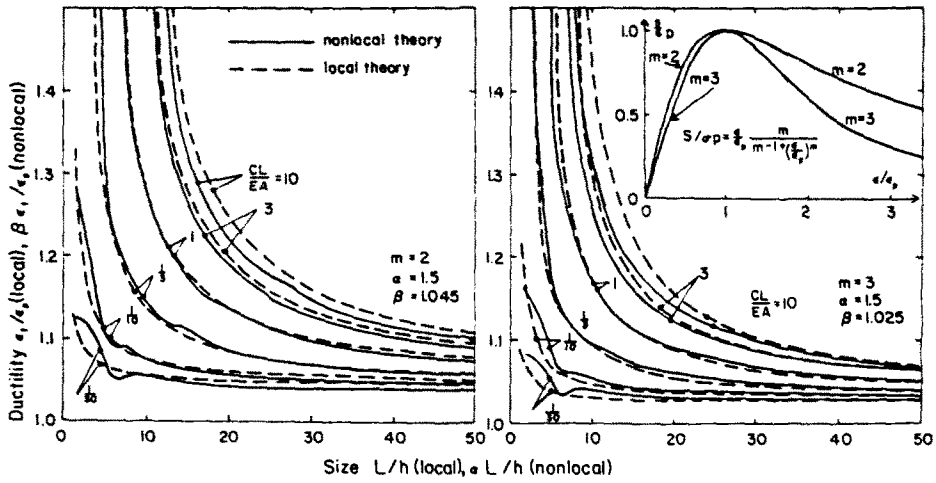

Fig. 5. Strain ε_f at strain-localization instability (ductility) as a function of bar length L for various spring constants C and various shapes of stress-strain diagram ($m = 2$ left, $m = 3$ right).

beam size, L/l. This again agrees with the assumptions made in the approximate blunt crack band model[2].

Figure 3(top) shows the effect of the ratio of the loading and unloading moduli E_t, E_u on the relative length of the strain-softening segment, $2h/l$, for the case of a relatively long bar, $L/h = 20$ (other properties being the same as before). In this diagram, the variation of the length of the strain-softening segment is somewhat more pronounced; $2h/l$ varies from 0.8 to 1.2. Note that in numerical calculations one must be careful to distinguish the first instability mode (solid curve in Fig. 3) from the second higher instability mode (the dashed curve in Fig. 3(top)). Only the first instability mode can occur in practice.

Figure 4 shows the stability limits in terms of spring constant C, normalized with regard to the unloading bar stiffness AE_u/L and plotted vs the ratio of loading to unloading moduli, $-E_t/E_u$.

Figures 5(a) and (b) show the ductility of the bar as a function of the relative bar length, L/l, for various values of spring constant C relative to the bar stiffness. The ductility is defined as the initial uniform strain in the bar at the onset of instability, ε_f, and its plot is normalized with regard to the strain ε_p at peak stress. The stress-strain diagram used in this calculation is given in Fig. 5(c), in which the formula is also written. The results are plotted for two values of m from this formula, corresponding to the typical post-peak response of low strength concrete ($m = 2$) and medium strength concrete ($m = 3$). The unloading modulus E_u is, in these calculations, assumed to be equal to the initial elastic modulus E, i.e. E_u is constant. This is done in order to make possible a comparison of the results with a previous solution based on the local crack band model[5]; these calculations were also made for $E_u = E = \text{const.}$ although it might have been more realistic to consider E_u to be a function of ε_f, such that E_u is between the secant modulus and the initial elastic modulus.

The diagrams in Figs 5(a) and (b) are plotted for various values of the spring constant C relative to the bar stiffness $E_u A/L$. We see that ductility generally decreases as the length of the bar increases, or as the spring stiffness decreases. These trends are well known from experiments.

The results previously obtained with the local solution based on the crack band model are shown for comparison as the dashed lines in Figs 4 and 5. The dashed lines in Fig. 5 were reported in previous work[4], in which it was shown that, in the local approach, the length of the strain-softening segment, h, must be considered to be a material property and, especially, must not be allowed to be arbitrarily small (this conclusion then led to the crack band theory in Refs [1, 5–7] for local finite element analysis of distributed cracking).

Although the length $h = w_c$ of the strain-softening segment in the local solution plays the same role as the characteristic length l or λ in the present non-local solution, there is

no reason why these two quantities should be exactly equal. Therefore, the length of the strain-softening segment (localization segment) in the local solution was considered as $w_c = l/\alpha$ where l is the characteristic length in the present non-local theory ($l^2 = 24\lambda^2$).

Similarly, the ductility values, i.e. the values of the strain ε_f at the onset of instability, do not have the same meanings in the local and non-local approaches, and so the strain at instability for the local solution was considered as $\beta\varepsilon_f$. The values of α and β were then varied so as to minimize the difference between the non-local and local solutions (in the least-square sense). Such best agreement is obtained for the present example when $\alpha = 1.5$ and $\beta = 1.045$ for $m = 2$ or $\beta = 1.025$ for $m = 3$ (Figs 5(a) and (b)). It is now worth noting that the differences between the local and non-local solutions in Figs 4 and 5(a) and (b) are indeed quite small, and that the optimum values of α and β are not very different from 1. We may thus conclude that the local solution, in which the length of the strain-softening segment (localization segment) is considered to be a material property (as is done in the blunt crack band theory), yields approximately correct results. A caveat must be added, though; this need not hold true for general three-dimensional solutions, in which boundary constraints or reinforcement might enforce the strain-softening region to be much larger than the characteristic length.

IMBRICATE NON-LOCAL BENDING THEORY

Another problem which is one-dimensional and easily amenable to an analytical solution is the non-local solution for bending. We consider a beam with a constant symmetric cross sectional area A and centroidal moment of inertia I (Fig. 1(g)). x, z are the axial and transverse coordinates and w the transverse deflection. We adopt the Bernoulli–Navier hypothesis that plane cross sections remain plane and normal to the deflection line and that transverse normal stresses are negligible. The deflections are assumed to be small. Introducing the relations $\bar{\varepsilon}(x) = \int \alpha(s)\varepsilon(x+s)\,\mathrm{d}s$, $\sigma = \bar{E}\bar{\varepsilon}$, $\tau = E\varepsilon$, $\varepsilon = \kappa z$, and $\bar{\varepsilon} = \bar{\kappa} z$, into the integrals $M = \int \sigma z\,\mathrm{d}A$, $m = \int \tau z\,\mathrm{d}A$, over the cross sectional area A, and defining the non-local and local bending moments, we obtain the relations

$$m = R\kappa, \quad M = \bar{R}\bar{\kappa}, \quad \kappa = w'', \quad \bar{\kappa}(x) = \int_{-l/2}^{l/2} \alpha(s)\kappa(x+s)\,\mathrm{d}s \tag{20}$$

where $R = EI$, $\bar{R} = \bar{E}I$, $I = \int z^2\,\mathrm{d}A$; $\bar{\kappa}$ is the non-local curvature, l the characteristic length of the non-local medium and $\alpha(s)$ the given weighting function, same as in eqns (1).

As a particularly simple strain-softening problem, we will analyze curvature localization in a simply supported beam shown in Fig. 1(g). Due to symmetry, the problem is equivalent to a cantilever beam of length L, loaded by a transverse distributed load q and at the end by a transverse concentrated load P. For the purpose of analytical solution, we again replace the integral averaging operator in eqns (20) by a differential operator, which is obtained by expanding $\kappa(x+s)$ into a Taylor series about point x. After truncation of higher-order terms, we thus obtain the approximation

$$\bar{\kappa} = w'' + \lambda^2 w^{\mathrm{IV}}. \tag{21}$$

We expect strain softening to occur within a symmetrically located segment of length $2h$ (Fig. 1(g)).

The virtual work expression for the bar may be written as

$$\delta W = \int_0^L [(1-c)M_1(\delta w_1'' + \lambda^2 \delta w_1^{\mathrm{IV}}) + cm_1\delta w_1'' - q\delta w_1]\,\mathrm{d}x + \int_h^L [(1-c)M_2(\delta w_2'' + \lambda^2\delta w_2^{\mathrm{IV}}) + cm_2\delta w_2'' - q\delta w_2]\,\mathrm{d}x - M\delta w'(L) - P\delta w_2(L) = 0 \tag{22}$$

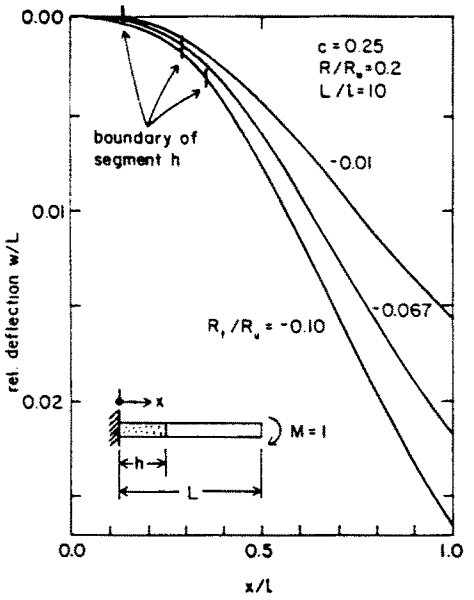

Fig. 6. Curves of deflection for various beam softening stiffnesses R_t.

which is similar to eqn (2) ($\lambda^2 = l^2/24$); q is the transverse distributed load. Subscripts 1 and 2 are affixed to distinguish between the segments of length h and $L-h$ (Fig. 6(b)).

The virtual work expression for the cantilever beam may be written as

$$\delta W = \int\int [(1-c)\sigma\delta\bar{\varepsilon} + c\tau\delta\varepsilon]\,\mathrm{d}A\,\mathrm{d}x - \int q\delta w\,\mathrm{d}x - M\delta w'(L) - P\delta w(L).$$

Substituting the previous expressions for ε and $\bar{\varepsilon}$, and splitting the integrals over segments of lengths h and $L-h$ (Fig. 6), we may rewrite this expression as

$$\begin{aligned}\delta W = {} & [(1-c)M_1(\delta w_1' + \lambda^2\delta w_1''') + cm_1\delta w_1']_0^h - [(1-c)M_1'(\delta w_1 + \lambda^2\delta w_1'') + cm_1'\delta w_1]_0^h \\ & + \int_0^h [(1-c)M_1''(\delta w_1 + \lambda^2\delta w_1'') + cm_1''\delta w_1 - q\delta w_1]\,\mathrm{d}x \\ & + [(1-c)M_2(\delta w_2' + \lambda^2\delta w_2''') + cm_2\delta w_2']_h^L - [(1-c)M_2'(\delta w_2 + \lambda^2\delta w_2'') + cm_2'\delta w_2]_h^L \\ & + \int_h^L [(1-c)M_2''(\delta w_2 + \lambda^2\delta w_2'') + cm_2''\delta w_2]\,\mathrm{d}x - M\delta w_2'(L) - P\delta w_2(L) = 0. \qquad (23)\end{aligned}$$

By two subsequent integrations by parts, eqn (22) may be transformed to

$$\begin{aligned}\delta W = {} & [\bar{M}_1\delta w_1']_0^h - [\bar{M}_1'\delta w_1]_0^h + (1-c)\lambda^2[M_1\delta w_1''' - M_1'\delta w_1'']_0^h \\ & + \int_0^h (\bar{M}_1'' - q)\delta w_1\,\mathrm{d}x + [\bar{M}_2\delta w_2']_h^L - [\bar{M}_2'\delta w_2]_h^L + (1-c)\lambda^2[M_2\delta w_2''' - M_2'\delta w_2'']_h^L \\ & + \int_h^L (\bar{M}_2'' - q)\delta w_2\,\mathrm{d}x - M\delta w_2'(L) - P\delta w_2(L) = 0 \qquad (24)\end{aligned}$$

with the notations

$$\bar{M}_1 = (1-c)(M_1+\lambda^2 M_1'')+cm_1, \quad \bar{M}_2 = (1-c)(M_2+\lambda^2 M_2'')+cm_2. \tag{25}$$

The condition that eqn (24) must be satisfied for any kinematically admissible variation $\delta w(x)$ yields:

the following differential equations of equilibrium

$$\bar{M}_1 = q, \quad \bar{M}_2'' = q; \tag{26}$$

the boundary conditions of symmetry at $x = 0$

$$\bar{M}_1\delta w_1'' = 0, \quad \bar{M}_1'\delta w_1 = 0, \quad M_1\delta w_1''' = 0, \quad M_1'\delta w_1'' = 0; \tag{27}$$

the interface conditions at $x = h$

$$\bar{M}_1\delta w_1' - \bar{M}_2\delta w_2' = 0, \quad \bar{M}_1'\delta w_1 - \bar{M}_2'\delta w_2 = 0, \quad M_1\delta w_1''' - M_2\delta w_2''' = 0,$$
$$M_1'\delta w_1'' - M_2'\delta w_2'' = 0; \tag{28}$$

the end boundary conditions at $x = L$

$$(\bar{M}_2 - M)\delta w_2' = 0, \quad (\bar{M}_2' - P)\delta w_2 = 0, \quad M_2\delta w_2''' = 0, \quad M_2'\delta w_2'' = 0. \tag{29}$$

From eqns (26) it is clear that $\bar{M}_1$ and $\bar{M}_2$ represent the total bending moments in the cross sections of the beam.

According to the particular kinematic conditions of our example (Fig. 1(g)), the boundary and interface conditions from eqns (27)–(29) reduce to:

for $x = 0$

$$w_1 = 0, \quad w_1' = 0, \quad w_1''' = 0, \quad M_1' = 0 \text{ (or } w_1^{V} = 0); \tag{30}$$

for $x = h$

$$w_1 = w_2, \quad w_1' = w_2', \quad w_1'' = w_2'', \quad w_1''' = w_2'''$$
$$\bar{M}_1 = \bar{M}_2, \quad \bar{M}_1' = \bar{M}_2', \quad M_1 = M_2, \quad M_1' = M_2'; \tag{31}$$

for $x = L$

$$w_2'' = 0, \quad w_2^{IV} = 0, \quad \bar{M}_2 = M_2, \quad \bar{M}_2' = P. \tag{32}$$

In view of eqn (21), the condition $M_1' = 0$ at $x = 0$ is equivalent to $w_1^{V} = 0$, as stated.

We now consider that the beam is initially in a stress state which involves strain softening within the central segment of length h. We are interested in the stability of this initial state and analyze, therefore, additional deformation increments. Thus, $w_1(x)$ and $w_2(x)$ represent small deflection increments from the initial state, and we assume $q = 0$.

To make an analytical solution feasible, we must assume that the bending rigidities R_t and R_u in segments h and $L-h$ are constant. This would not be possible if the properties of the beam were defined by stress–strain relations, because, in contrast to our previous analysis of the bar, the initial distribution of the bending moment is not uniform (Fig. 1(h)). Therefore, we assume that the beam properties are characterized by local and non-local moment curvature relations which exhibit strain softening. Even though the initial bending moment is nonuniform over the beam, we assume that the incremental bending rigidities R_t and R_u for further loading and for unloading are constant within the range of initial bending moments in the segments h and $L-h$ (Fig. 1(i)).

Strain softening may be exhibited only by the non-local moment curvature relation between M and $\bar{\kappa}$. The local moment curvature relation between m and κ (Fig. 1(j)) is assumed to be elastic, with bending rigidity R. Substituting $M_1 = R_t w_1''$, $M_2 = R_u w_2''$,

$m_1 = Rw_1''$, $m_2 = Rw_2''$ into eqns (25) and then into eqns (26), we obtain the basic differential equations of the problem

$$M_1'' = (1-c)R_t(w_1'' + 2\lambda^2 w_1^{IV} + \lambda^4 w_1^{VI})'' + cRw_1^{IV} = q$$
$$M_2'' = (1-c)R_u(w_2'' + 2\lambda^2 w_2^{IV} + \lambda^4 w_2^{VI})'' + cRw_1^{IV} = q. \quad (33)$$

The present problem is mathematically equivalent to the previous problem of axial deformation. Indeed, if we replace w'' by u, eqns (33) become identical to eqns (9). Thus, the general analytical solution is of the same form, except that two more integrations must be carried out to obtain w from w''. The general solution of the differential equations in eqns (33) for the softening segment of length h and the non-softening segment of length $L-h$ is

$$w_1(x) = B_1 \sin \alpha_1 x + B_2 \sin \beta_1 x + B_3 \sin \alpha_1 x + B_4 \cos \beta_1 x + B_5 x^3 + B_7 x + B_8 \quad (34)$$

$$w_2(x) = C_1 \cosh \alpha_2 x \sin \beta_2 x + C_2 \sinh \alpha_2 x \cos \beta_2 x + C_3 \cosh \alpha_2 x \cos \beta_2 x + C_4 \sinh \alpha_2 x \sin \beta_2 x + C_5 x^3 + C_6 x^2 + C_7 x + C_8 \quad (35)$$

in which

$$\alpha_1 = \lambda^{-1}(1+A_1)^{1/2}, \quad \beta_1 = \lambda^{-1}(1-A_1)^{1/2}, \quad A_1 = (cR)^{1/2}[-(1-c)R_t]^{-1/2} \quad (36)$$

$$\alpha_2 = \lambda^{-1}(A_3 - \tfrac{1}{2})^{1/2}, \quad \beta_2 = \lambda^{-1}(A_3 + \tfrac{1}{2})^{1/2}, \quad A_3 = [\tfrac{1}{2}(1+A_2)]^{1/2}, \quad A_2 = cR[(1-c)R_t]^{-1}. \quad (37)$$

This solution involves 16 unknown constants, for which the boundary conditions and the interface conditions in eqns (30)–(32) yield 16 linear algebraic equations.

CURVATURE LOCALIZATION INSTABILITY AND NUMERICAL RESULTS

Based on the foregoing formulation, we may now study the conditions under which strain-softening behavior in a beam becomes unstable. Similar to our previous procedure for axial deformations in a bar, we consider that an incremental load is applied at the cantilever end (Fig. 1(g)), either $P = -1$ or $M = -1$. Then we scan the range of values of $|R_t|/R_u$ and h/L. We choose a series of discrete values of these variables, solve the problem for each combination and calculate for the beam end the displacement $w_2(L)$, where an end load is considered, or $w_1'(L)$ when an end moment is considered. If this value is positive, the beam is stable, and if it is negative, the beam is unstable. The smallest value of $|R_t|/R_u$ for which this happens for some value of h is the critical state.

The numerical results are shown in Figs 6 and 7 and the bottom of Fig. 3. Figure 3(bottom) shows the length of the curvature localization zone h as a function of the softening bending rigidity. The steeper the softening slope, the longer is the strain-softening segment. For steep softening slopes, the ratio $2h/l$ seems to be almost constant and equal to 0.8. Figure 6 shows the deflection curves of the cantilever beam for the applied moment at the end ($M = -1$). The deflection curves are plotted in Fig. 6 for three stiffness ratios. Note that a steeper softening slope causes an increase of the deflection. The distributions of the

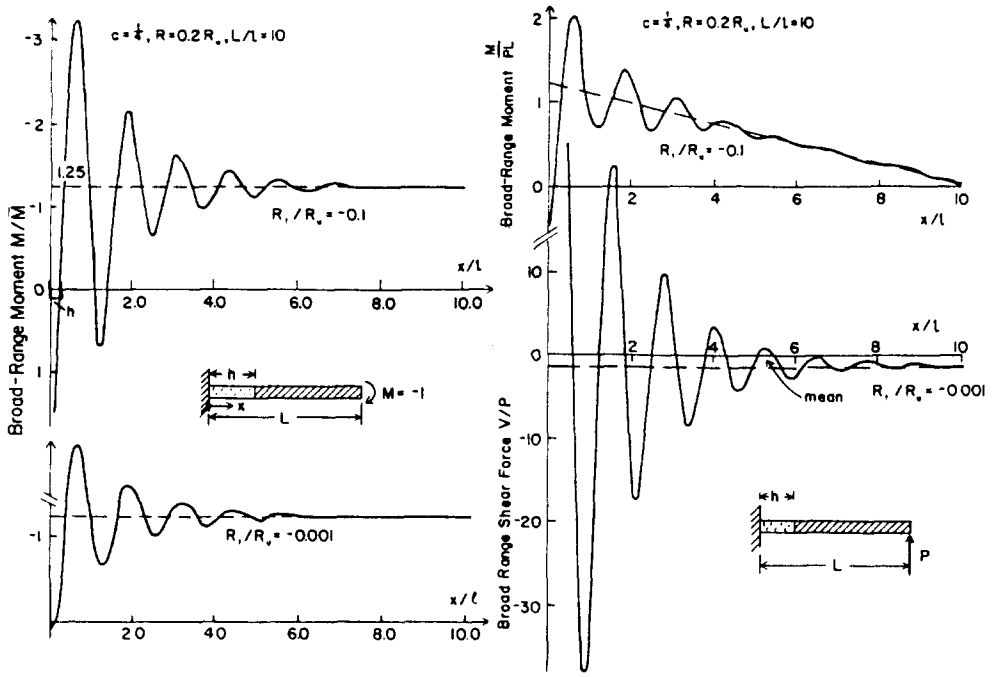

Fig. 7. Distributions of broad-range bending moment M and shear force V for various softening stiffnesses and load cases.

ratio of the broad-range moment M to the total moment $\bar{M}$ (Fig. 7(left)) indicate that the deviation from the local solution (horizontal dashed lines) increases significantly with the softening slope R_t.

The same cantilever beam was subjected at the free end to the transverse force $P = -1$ (Fig. 7(right)). In this case one finds that the plot of the softening zone length h vs R_t/R_u is almost identical with the previously obtained plot for $M = -1$ (Fig. 3(bottom)). The diagrams of deflection w/l within the short softening segment are also nearly identical. Figure 7 shows the distributions of broad-range bending moment M and broad-range shear force V. Note that for a very small softening slope, $R_t/R_u = -0.001$, the distribution of M and especially V significantly deviate from the local solution (dashed lines) for small x, but for larger x gradually converge to them.

CONCLUSIONS

(1) The differential approximation of imbricate non-local continuum permits modeling strain-softening regions in bars and beams which are of a finite length, and it makes possible an exact analytical solution.

(2) The essential and natural boundary conditions are derived by a consistent variational procedure from the principle of virtual work.

(3) Similar to previous work[4], the failure due to strain softening is treated as a stability problem of a continuous structure.

(4) The previously published solution based on a local continuum concept and a size limitation on the strain-localization zone yields approximately the same results as the present exact solution. This lends further justification to the blunt crack band model for distributed cracking.

(5) In the present formulation, the length of the softening segment is not specified in advance but is unknown; it may be determined by stability analysis. This length appears to be approximately constant over a broad range of conditions and approximately the same as the width of the strain-softening region (cracking zone) in the aforementioned previous local approach. The energy dissipated due to strain softening seems to be also almost the same for these two approaches.

Acknowledgement—Partial financial support under NSF grant No. MSM-8700830 to Northwestern University is gratefully acknowledged.

REFERENCES

1. Z. P. Bažant, Mechanics of distributed cracking. *ASME Appl. Mech. Rev.* **39**(5), 675–705 (1986).
2. Z. P. Bažant, T. P. Chang and T. B. Belytschko, Continuum theory for strain-softening. *J. Engng Mech. ASCE* **110**, Dec. (1984).
3. Z. Mróz, Current problems and new directions in mechanics of geomaterials. In *Mechanics of Geomaterials (Proc. of IUTAM Prager Symp.*, Northwestern Univ., Sept. 1983) (Edited by Z. P. Bažant), pp. 539–566. Wiley, New York (1985).
4. Z. P. Bažant, Instability, ductility and size effect in strain-softening concrete. *J. Engng Mech. Div. ASCE* **102**, 331–344 (1976); Discussions. *J. Engng Mech. Div. ASCE* **103**, 357–358, 775–777; **104**, 501–502, based on Struct. Engng Report No. 74-8 640, Northwestern University, Aug. (1974), and private communication to K. Gerstle, S. Sture and A. Ingraffea, Boulder, Colorado, 5 June (1974).
5. Z. P. Bažant, Crack band model for fracture of geomaterials. *Proc. 4th Int. Conf. on Numerical Methods in Geomechanics*, University of Alberta, Edmonton (Edited by Z. Eisenstein), Vol. 3, pp. 1137–1152 (June 1982).
6. Z. P. Bažant and L. Cedolin, Blunt crack band propagation in finite element analysis. *J. Engng Mech. Div. ASCE* **106**(EM6), 1287–1306 (1980).
7. Z. P. Bažant and B. H. Oh, Crack band theory for fracture of concrete. *Matér. Construct.* (*RILEM, Paris*) **16**(93), 155–177 (1983).
8. A. Hillerborg, M. Modéer and P. E. Petersson, Analysis of crack formation and crack growth in concrete by means of fracture mechanics and finite elements. *Cem. Concr. Res.* **6**(6), 773–782 (1976).
9. G. I. Barrenblatt, The formation of equilibrium cracks during brittle fracture, general ideas and hypothesis, axially symmetric cracks. *Prikl. Mat. Mekh.* **23**(3), 434–444 (1959).
10. D. S. Dugdale, Yielding of steel sheets containing slits. *J. Mech. Phys. Solids* **8**, 100–108 (1960).
11. A. C. Eringen and D. G. B. Edelen, On nonlocal elasticity. *Int. J. Engng Sci.* **10**, 233–248 (1972).
12. E. Kröner, Interrelations between various branches of continuum mechanics. In *Mechanics of Generalized Continua* (Edited by E. Kröner), pp. 330–340. Springer, Berlin (1968).
13. J. A. Krumhansl, Some considerations of the relation between solid state physics and generalized continuum mechanics. In *Mechanics of Generalized Continua* (Edited by E. Kröner), pp. 298–331. Springer, Berlin (1968).
14. I. A. Kunin, The theory of elastic media with microstructure and the theory of dislocations. In *Mechanics of Generalized Continua* (Edited by E. Kröner), pp. 321–328. Springer, Berlin (1968).
15. V. M. Levin, The relation between mathematical expectation of stress and strain tensors in elastic micro-heterogeneous media. *Prikl. Mat. Mekh.* **35**, 694–701 (1971), in Russian.
16. Z. P. Bažant, F. Lin and G. Pijaudier-Cabot, Yield limit degradation: nonlocal continuum model with local strain. *Proc. Int. Conf. on "Computational Plasticity"* (Edited by D. R. J. Owen, E. Hinton and E. Oñate), pp. 1757–1780. Barcelona, Spain (April 1987).
17. Z. P. Bažant and G. Pijaudier-Cabot, Modeling of distributed damage by nonlocal continuum with local strain. *Proc. Fourth Int. Conf. on "Numerical Methods in Fracture Mechanics"* (Edited by A. R. Luxmoore, D. R. J. Owen, Y. P. S. Rajapakse and M. F. Kanninen), pp. 411–432. San Antonio, Texas (March 1987).
18. G. Pijaudier-Cabot and Z. P. Bažant, Nonlocal damage theory. *J. Engng Mech. ASCE* **113**(10), 1512–1533 (1987).
19. Z. P. Bažant, Imbricate continuum: variational formulation. Report No. 83-11/428i, Center for Concrete and Geomaterials, Northwestern University, Evanston, Illinois; also *J. Engng Mech. ASCE* **110**(10), 1693–1712 (1983).